21cm Intensity Mapping + kSZ Effect: a Handy Probe for Larger Scale, Wider Redshift Baryon Distributions

Dongzi Li,[1,2] Ue-Li Pen,[3,4,5,1] Hong-Ming Zhu,[6,7] and Yu Yu[8]

[1]*Perimeter Institute for Theoretical Physics, 31 Caroline St. N., Waterloo, ON, N2L 2Y5, Canada*
[2]*University of Waterloo, 200 University Ave W, Waterloo, ON, N2L 3G1, Canada*
[3]*Canadian Institute for Theoretical Astrophysics, 60 St. George Street, Toronto, Ontario M5S 3H8, Canada*
[4]*Dunlap Institute for Astronomy and Astrophysics, 50 St. George Street, Toronto, Ontario M5S 3H4, Canada*
[5]*Canadian Institute for Advanced Research, CIFAR Program in Gravitation and Cosmology, Toronto, Ontario M5G 1Z8, Canada*
[6]*Key Laboratory for Computational Astrophysics, National Astronomical Observatories, Chinese Academy of Sciences, 20A Datun Road, Beijing 100012, China*
[7]*University of Chinese Academy of Sciences, Beijing 100049, China*
[8]*Key Laboratory for Research in Galaxies and Cosmology, Shanghai Astronomical Observatory, Chinese Academy of Sciences, 80 Nandan Road, Shanghai 200030, China*

(Dated: December 27, 2016)

The prominent defficiency of baryons in observations at $z \lesssim 2$ and its poorly understood relationship with stellar feedback and the local conditions of the intergalactic medium stand in the way of understanding the evolution of structure in the universe. The kinematic Sunyaev-Zel'dovich (kSZ) distortion of the Cosmic Microwave Background (CMB) has been proposed as a method for measuring these diffuse "missing baryons" on large-scales. However, the faintness and lack of redshift information of the method limit its usefulness, suggesting cross-correlation with another probe. Previous proposals require the combination of spectroscopic galaxy surveys with new generation ground based CMB experiments to obtain convincing signal-to-noise (S/N). This limits the redshift depth and sky coverage they could reach. In this paper, the new possibility of cross-correlating kSZ with the neutral hydrogen (HI) density from 21 cm intensity mapping is discussed and tested with simulations. Ongoing experiments, such as CHIME, will, in next few years, measure the HI distribution at $z \lesssim 2.5$ over large fractions of the sky. The greatest challenge for our method is the loss of large-scale 21 cm modes due to the combined effects of foreground filtering and spatial loss of interferometers related to shortest baselines. We alleviate this problem by restoring the large scale modes from its tidal influence on small scales. A minimum S/N of 15 for both redshifts 1 and 2 could be reached with a cross-correlation of CHIME and Planck. Interferometers with longer baselines, such as HIRAX, will be able to produce S/N reaching ~ 30 for redshift 1 and ~ 50 for redshift 2.

PACS numbers:

I. INTRODUCTION

For $z \lesssim 2$, a large fraction of the predicted baryon content is missing in observations. The majority of these baryons are believed to reside in the warm-hot intergalactic medium (WHIM), with typical temperatures of 10^5 K to 10^7 K [1, 2]. Its high temperature and associated low density impose difficulties for direct detection. Furthermore, the uncertainty in the spatial distribution of its ionization state, metalicity, and pressure lead to confusion in interpreting signals from absroption lines and soft X-rays. There is therefore an urgency for probes that not only trace the majority of the missing baryons, but also can be interpreted model-independently.

Among proposed probes, the kinematic Sunyaev-Zel'dovich (kSZ) effect [3–5] is a promising one. The kSZ effect results from Compton scattering of Cosmic Microwave Background (CMB) photons off of free electrons. The radial velocity of the electrons provides a Doppler shift to the photons causing a secondary anisotropy in CMB temperature. It is an ideal probe to tackle the missing baryon problem: First, it recieves a contribution from all the free electrons. For low redshift, $\gtrsim 90\%$ of baryons are in ionized states [6], and can be traced by free electrons. Second, the signal is mainly influenced by the electron density and radial velocity, regardless of the temperature, pressure, and metalicity, so no extra assumptions are needed to estimate the baryon abundance. Third, the dominant piece of the peculiar velocity signal comes from the large-scale structure, and therefore the signal is less biased by the local environment, and more indicative of the diffuse distribution.

Attractive as it is, two drawbacks largely reduce the feasibility of harnessing the kSZ signal. First, the signal is weak compared to the primary CMB anisotropies and hence suffers seriously from contaminations from the primary, instrumental noise, the thermal SZ effect, CMB lensing, etc ... Second, it is an integrated effect along the line of sight and does not contain redshift information.

Cross correlation of the kSZ signal with another tracer, which has both large-scale structure and redshift information, provides a straight-forward mitigation of these disadvantages. Previous work has proposed optical spectroscopic surveys as an ideal tool [7–9]. However, the lack of prominent spectral lines at redshift $1.4 - 2.5$ makes it difficult to consistently measure evolution from $z = 2$ to $z = 0$. Moreover, the difficult technical specifications required for source detection, especially at high redshift, largely constrain the sky coverage and limit such surveys to relatively small angular scales, where the power from the primary CMB is low. Methods with lower requirements on facilities such as cross-correlation of photo-z galaxies with kSZ [10, 11], depend on models of velocity fields and demand next generation CMB facilities, such as ACTpol,

CMB-S4, to achieve convincing S/N.

In this paper, the new possibility of cross-correlating the neutral hydrogen (HI) density field from 21 cm intensity mapping (IM) experiments with the kSZ signal is discussed and tested with simulations. The redshifted 21 cm line provides accurate redshift information, which will soon be available at $z \lesssim 2$. Intensity mapping surveys, rather than distinguishing individual galaxies, integrate all signals in a pixel, enabling them quickly scan large areas of the sky. In the following few years, there will be several full-sky experiments producing data at redshifts $\lesssim 2.5$ [12–14]. With the abundant data of density fields with accurate redshift information, we are able to linearly reconstruct the velocity fields, and hence calculate a large sky kSZ map to cross correlate with real kSZ signals.

Promising as it seems, the loss of large-scale modes in IM surveys will complicate the cross-correlation of the IM field with kSZ signals. The main challenge comes from the bright astrophysical foregrounds, which contaminate the large-scale modes parallel to the line of sight, i.e. small $k_\parallel$ modes. Besides, the large-scale modes in perpendicular plane, i.e. small $k_\perp$ modes, is poorly resolved with inteferometers. Fig.1 shows an illustration of the modes of the matter density field which can be observed by a CHIME-like survey. Since the large scale modes are essential for calculating velocity fields, directly using this IM fields to cross correlate with kSZ signal can only resolve $< 20\%$ of the signal.

Therefore, in this work, we first solve for the large-scale modes from their non-linear tidal distortions on small scale power spectrum [15, 16]. As shown in simulations, velocity fields can be well reproduced after the algorithm. Convolving the reconstructed v_z with large ℓ density fields, we could better assemble observable kSZ signals. The full procedure is depicted at the bottom of Fig. 1. The effect on the cross-correlation obtained from this method of varying various survey-related parameters such as foreground noise level, shortest baseline length, spatial and frequency resolution are discussed.

The paper is organized as follows: Section II introduces the method we use to cross-correlate density fields with the kSZ signal (similarly to [8]); Section III discusses the realities of 21cm IM surveys and properties of the observed fields; Section IV clarifies the important scales of the density and velocity fields in relation to the kSZ signal; Section IV describes the non-linear tidal reconstruction method for the missing large-scale modes in the IM fields; Section V presents our analytical and numerical results, while in Section VI we summarize our S/N calculations; We conclude in Section VII.

II. CROSS-CORRELATION OF DENSITY FIELDS WITH KSZ

The CMB temperature fluctuation caused by the kSZ effect is simply a line-of-sight integral of the free electron momentum field:

$$\Theta_{\rm kSZ}(\boldsymbol{n}) \equiv \frac{\Delta T_{\rm kSZ}}{T_{\rm CMB}} = -\frac{1}{c}\int d\eta g(\eta) p_\parallel(\eta, \boldsymbol{n}) \,, \qquad (1)$$

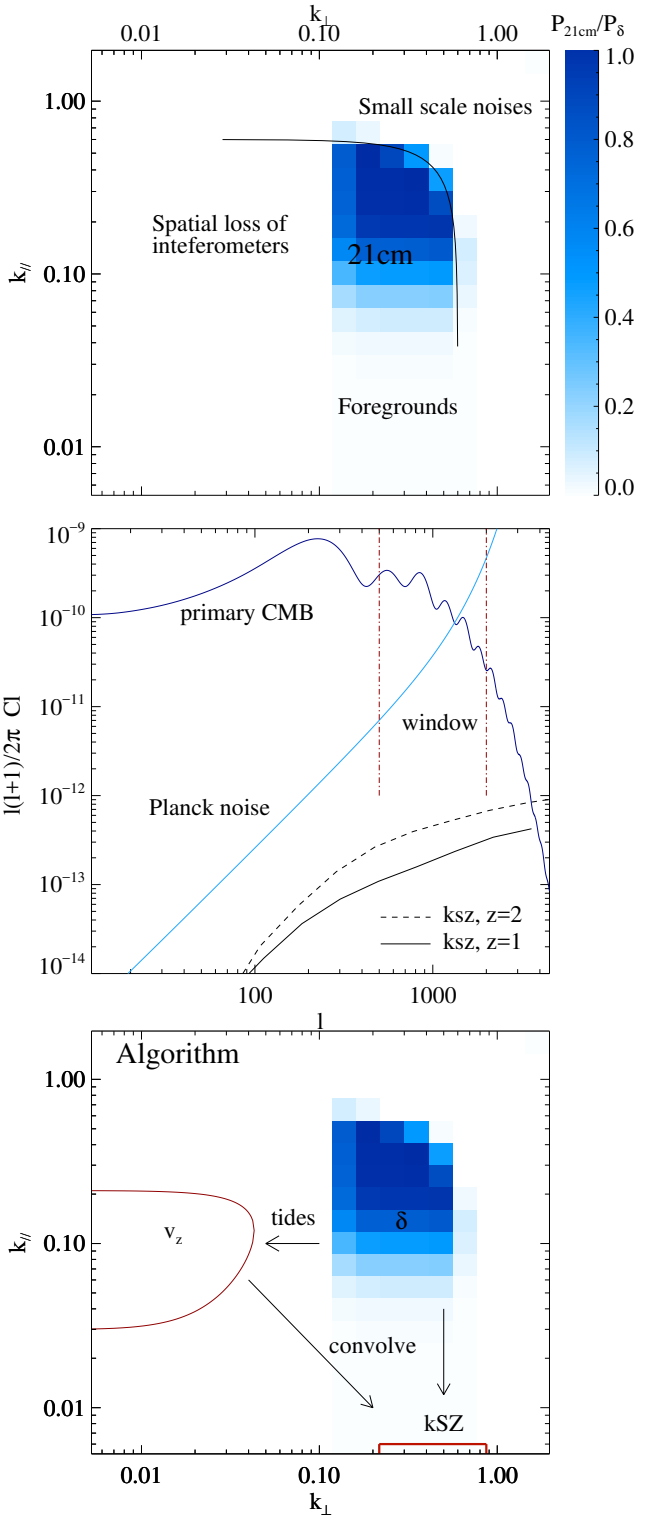

FIG. 1: (Top) Theoretical prediction for the two-dimensional power spectrum of 21 cm fluctuations at $z = 1$ observed by CHIME, assuming high foregrounds ($R_\parallel = 15$ h/Mpc). See discussions in Section.III. (Middle) Window for kSZ measurements based on Planck 217 GHz band noise. The kSZ signal is calculated in 1.2 Gpc boxes. (Bottom) The algorithm could be divided into two parts: 1. solving for the lost large scale modes from their tidal distortions on small scale power spectra observed in 21cm IM; 2. calculating the velocity fields from reconstructed large scale modes and multiply them with density fields in real space. Notice that the multiplication in real space is a convolution in Fourier space, therefore the effective modes for velocity and density fields are off by $\ell \sim 1000 - 2000$ in projected plane. See discussions in

where $\eta(z)$ is the comoving distance, $g(\eta) = e^{-\tau} d\tau/d\eta$ is the visibility function, τ is the optical depth to Thomson scattering, $p_\parallel = (1+\delta_e)v_\parallel$ is the momentum field parallel to the line of sight, and $\delta_e = (\rho - \bar{\rho})/\bar{\rho}$ is the free electron overdensity, with $\bar{\rho}$ denoting the average density. It is assumed that electron overdensity δ_e is closely related to baryon overdensity at $z < 2$, therefore we simply use δ to denote both hereafter.

The direct correlation between kSZ and density fields vanishes due to the cancellation of positive and negative velocities. A holographic to avoid the cancellation is to reconstruct the peculiar velocity fields v_z and convlove them with density fields at each redshift.

From the linearized continuity equation:

$$v_z(\boldsymbol{k}) = iaHf\delta(\boldsymbol{k})\frac{k_z}{k^2} \tag{2}$$

where a is the scale factor, $f = d\mathrm{ln}D/d\mathrm{ln}a$, $D(a)$ is the linear growth function, H is the Hubble parameter, z is the direction parallel to the line of sight.

Now it is possible reconstruct the 2D kSZ field for a specific redshift bin with v_z and δ following Eq (1). To quantify the tightness of correlation between reconstructed kSZ and real kSZ, we introduce a correlation coefficient r:

$$r \equiv \frac{P_{\mathrm{recon,real}}}{\sqrt{P_{\mathrm{recon}}P_{\mathrm{real}}}} \tag{3}$$

where $P_{\mathrm{recon,real}}$ is the cross power spectrum.

III. CHALLENGES FOR 21 CM INTENSITY MAPPING

Ideally, the velocity reconstruction method diskussed in the previous section should retrieve a $> 90\%$ cross-correlation with the real kSZ signal [8]. However, realistic 21 cm IM experiments can only detect density fluctuations at certain scales, as illustrated in Fig.1. Three main factors lead to the loss of modes.

1. The angular resolution of the telescope:

   In comparison to galaxy surveys, IM surveys sacrifice angular resolution in exchange for sky coverage and survey speed. The effect of this finite angular resolution on S/N of the cross-correlation can be roughly taken in to account with a Heaviside Function in $k_\perp$ space, $H(k_{\mathrm{max}} - k)$.

2. Foreground noise level:

   Foregrounds from Galactic emission, extragalactic radio sources and Radio recombination lines, together with the noise of the telescope could be three orders brighter than the targeted signal [17, 18]. The process of foreground removal, which takes advantage of the low spectral degrees of freedom of the forgegrounds [19], requires the removal of the corresponding large-scale structure in the radial direction, as well. To imitate the loss, we apply a high pass filter $W(k_\parallel) = 1 - e^{-k_\parallel^2 R_\parallel^2/2}$.

	z=1		z=2	
	high foreground	low foreground	high foreground	low foreground
$R_\parallel$ Mpc/h [a]	15	60	10	40
	CHIME	HIRAX	CHIME	HIRAX
k_{max} h/Mpc [b]	0.6	1.2	0.4	0.8
ℓ_{min} [c]	300			

[a] Foreground: filter out $k_z \lesssim 0.08, 0.02, 0.12, 0.03$ h/Mpc respectively. Parameters based on [20–22]

[b] Small scale noise: based on CHIME[12] and HIRAX[14] with 80 m and 200 m longest baseline respectively.

[c] Spatial loss of inteferomenter: assuming shortest baseline of 20 m.

TABLE I: Parameters related to resolvable modes in 21cm IM

3. The shortest baseline of inteferometers:

   Current 21cm IM experiments are all carried on inteferometers. For CHIME-like facilities, with multiple beams installed on one disk, the calibration for cross correlation between two beams of the same disk are complicated. Therefore, we only consider results from cross correlating signals from distinct disks. Then the minimum spacing between disks is the shortest baseline, which decides the largest angular scale it could probe. We again use a Heaviside function $H(\ell - \ell_{\mathrm{min}})$ to mimick this effect.

Therefore, a realistic 21 cm density contrast will appear as

$$\delta_{\mathrm{IM}}(\boldsymbol{k}) = \delta(\boldsymbol{k})H(k_{\mathrm{max}} - k)W(k_\parallel)H(\ell - \ell_{\mathrm{min}}). \tag{4}$$

where $k_\parallel = \ell/\chi$.

Table.I lists several representive values for the different parameters introduced above, based on previous observations and predictions. Fig. 1 is an illustration of the relevant scales for the various observables, corresponding to $R_\parallel = 15$ Mpc/h, $k_{\mathrm{max}} = 0.6$ h/Mpc at $z = 1$. With this 21 cm IM field, we construct a momentum field $p_\parallel$ following Eq.(1). As demonstrated in Fig.2, it does not cover the modes necessary for a cross-correlation with kSZ.

Actually, directly using δ_{IM} with any combination of the parameters above to generate kSZ map will only yield a correlation coeffcient $r < 0.2$ with observable kSZ signals.

IV. IMPORTANT SCALES FOR KSZ SIGNALS

To understand which $\boldsymbol{k}$ of δ are most necessary in reconstructing the kSZ signal, the first step is to clarify which angular scale of the kSZ we are interested in. As demonstrated in Fig.1, the kSZ effect is too faint to be distinguished until the primary CMB starts to fade away, at roughly $\ell > 500$. It is possible to select a frequency band where the thermal SZ signal is negligible, then the dominant factor at high ℓ will be the CMB instrumental noise. With existing Planck [23] data at 217 GHz, $\ell \sim 500 - 3000$ will be the visible window for kSZ signal to be distinguished with sufficient S/N over primary CMB and facility noise. The way to estimate S/N is presented in Section.VII. The window could be extended to higher frequency with ACTpol and CMB-S4.

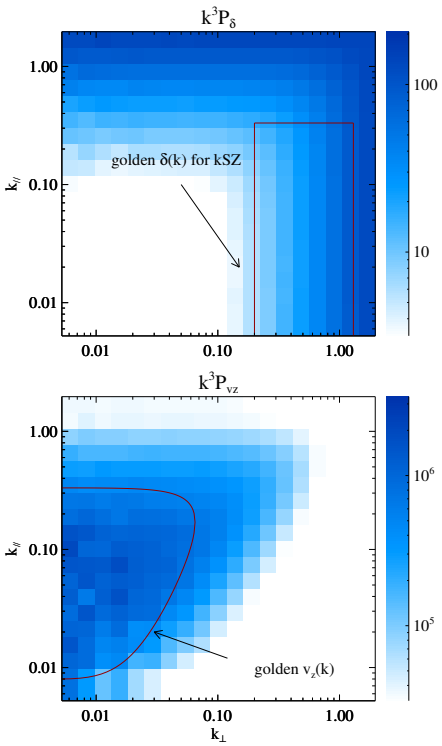

FIG. 2: The variances $2\pi^2\Delta^2 \equiv k^3P$ indicate how Fourier modes of different scales contribute to real space fields, i.e. $\delta(\boldsymbol{x})$ and $v_z(\boldsymbol{x})$. The modes essential for generating kSZ signals at $\ell \sim 500 - 3000$ are marked out as "Golden modes".

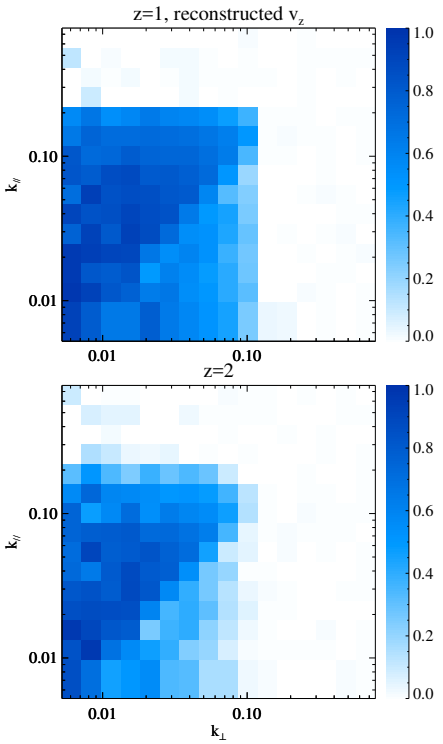

FIG. 3: The correlation coefficient between the reconstructed v_z and actual v_z, assuming the longest baseline of 80 m with foregrounds seriously contaminate k_z below ~ 0.08 h/Mpc and ~ 0.12 h/Mpc at $z = 1$ & 2, respectively

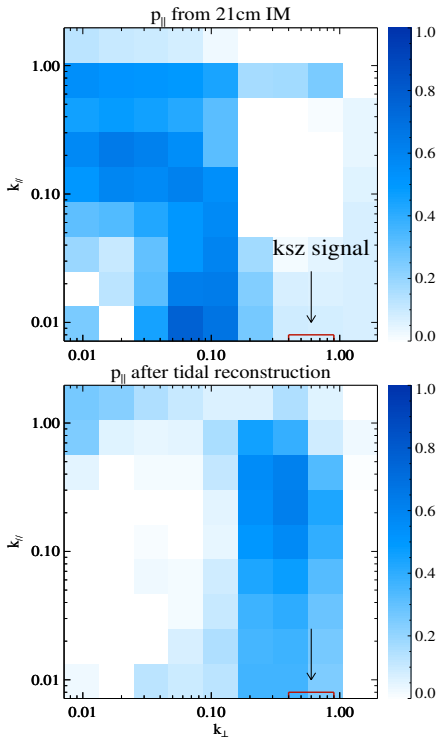

FIG. 4: The correlation coefficient between actual momentum fields $p_\parallel = (1+\delta)v_z$ and momentum fields reconstructed from IM fields before and after tidal reconstruction. The kSZ signal is roughly $p_\parallel$ integrated over line of sight, corresponding to $k_z = 0$ modes. [Titles should say correlation coefficient of . . . or have no title.]

The next step is to understand what role each scale plays in contributing to the kSZ signal at $\ell \sim 500 - 3000$. If we write Eq.(1) in Fourier space, and given that $g(\eta)$ varies slowly, we see that $\Theta(\boldsymbol{\ell})$ is propotional to the $k_z = 0$ mode of the momentum field, as marked in Fig.2,

$$\Theta(\boldsymbol{\ell}) \propto p_\parallel(k_x\chi, k_y\chi, 0) \propto \int d^3k'\, \delta(\boldsymbol{\ell}/\chi - \boldsymbol{k}'_\perp, k'_\parallel) v_z(\boldsymbol{k}'_\perp, k'_\parallel). \quad (5)$$

The convolution of δ and v_z tells us that the signal comes from the cross talk of $\boldsymbol{\ell}/\chi - \boldsymbol{k}'_\perp$ and $\boldsymbol{k}_\perp$, with a sum over all k'.

Although the summation is over all k', not all the modes make conceivable contributions to final signal $\Theta(\boldsymbol{\ell})$. The effective modes on velocity and density fields for generating kSZ signals should satisfy two requirements: 1. Since the two fields are fully coupled together, only when $|\delta|$ and its coupling partner $|v_z|$ are both sufficiently large can they make noticeable contribution to $\theta(\boldsymbol{\ell})$; 2. The convolution in Eq (5) indicates that not $v_z(\boldsymbol{k})$ and $\delta(\boldsymbol{k})$ with identical $\boldsymbol{k}$, but those with identical k_z but a seperation of $\delta\boldsymbol{k}_\perp = \ell/\chi$ in $k_\perp$ plane can be coupled together. Therefore, the effective modes for v_z and δ come as a pair with ℓ seperation in k space.

Having these two factors in mind, we look at the relative strength of different modes in v_z and δ in Fig.**??**. The modes circled by red lines in upper and lower panels are coupled together, and both components in a pair have enough power. These are the effective modes for generating kSZ signals.

Another way to look at this is to boldly approximate v_z as a Dirac delta function $\delta^D(\boldsymbol{k}')$, since $v_z \propto k_z/k^3$, its power drops fast as k grows. Then $\Theta(\boldsymbol{\ell})$ will reduce to $\delta(\boldsymbol{\ell}/\chi, 0)v_z(0,0)$, with integration over the other k' being negligible due to the faintness of $v_z(k' \neq 0)$. In reality, where $v_z(\boldsymbol{k})$ is not as sharp as a Dirac delta, the peak will be closer to $(k_\perp,k_\parallel)$=(0.01,0.1) h/Mpc rather than (0,0). We then see that most of the kSZ signal is generated by the cross talk between the part of $v_z(\boldsymbol{k})$ with k in a small ball surrounding (0.01,0.1) h/Mpc and the part of $\delta(k)$ with k close to $\delta(\boldsymbol{\ell}/\chi, 0.1)$ h/Mpc. This is identical to previous estimates. Comparing the effective modes for generating kSZ signals with modes resolved in 21cm IM in Fig.1, we notice that while the effective modes for δ are partly resolved, the large scale information dominating v_z is almost completely filtered out of the 21 cm IM field. Therefore, to

retrieve the cross-correlation between kSZ and 21cm IM fields we must first reconstruct the large-scale v_z modes.

V. COSMIC TIDAL RECONSTRUCTION

Until now only linear theory has been considered in the reconstruction. However, to extract the lost large-scale information, we need to consider couplings between different scales which arise in non-linear perturbation theory. Here, we present the algorithm we use to solve for the large-scale structure, based on tidal couplings [15, 16].

The evolution of small-scale structure is modulated by large-scale tidal forces. Consider only the anisotropic influence from tidal force, the generated distortions on matter power spectrum will be

$$\Delta P(\boldsymbol{k},\tau)|_{t_{ij}} = \hat{k}^i \hat{k}^j t_{ij}^{(0)} P_{1s}(k,\tau) f(k,\tau), \tag{6}$$

where $P_{1s}(k,\tau)$ is the linear power spectrum, $f(k) = 2\alpha(\tau) - \beta(\tau) d\ln P/d\ln k$ is the tidal coupling function, with α and β parameters related to the linear growth funcion [16]. For example, $(\alpha,\beta) = (0.6, 1.3)$ and $(0.4, 0.9)$ for $z = 1$ and $z = 2$, respectively. t_{ij} is the tidal force tensor, which is symmetric and traceless and hence can be decomposed into five independent observables:

$$t_{ij} = \begin{pmatrix} \gamma_1 - \gamma_z & \gamma_2 & \gamma_x \\ \gamma_2 & -\gamma_1 - \gamma_z & \gamma_y \\ \gamma_x & \gamma_y & 2\gamma_z \end{pmatrix}. \tag{7}$$

Therefore, from the spatial dependence of the distortions $\Delta P(\boldsymbol{k},\tau)$, we can solve for different components of t_{ij}. The tidal forces are related to second derivative of large scale gravitational potential Φ_L,

$$t_{ij} = \partial_i \partial_j \Phi_L - \nabla^2 \Phi_L \delta_{ij}/3/, \tag{8}$$

where δ_{ij} is the Kronecker delta function.

Different components of t_{ij} are related to different k modes of the large-scale density contrast κ_{3D}.

$$\kappa_{3D} = \nabla^2 \Phi_L = \frac{3}{2} \nabla^{-2} \partial_i \partial_j t_{ij} \tag{9}$$

We note that $f(k,\tau)$ increases with k at the scales we are interested in, indicating the distortions are more manifest on small scales. This reinforces the feasibility of using observable high k modes of the 21 cm IM field to extract low k modes.

VI. SIMULATIONS AND RESULTS

To test the algorithm, we performed six N-body simulations, using the CUBEP^{3}M code [24], each evolving 1024^3 particles in a $(1.2\mathrm{Gpc}/h)^3$ box. Simulation parameters are set as: Hubble parameter $h = 0.678$, baryon density $\Omega_b = 0.049$, dark matter density $\Omega_c = 0.259$, amplitude of primordial curvature power spectrum $A_s = 2.139 \times 10^{-9}$ at $k_0 = 0.05\ \mathrm{Mpc}^{-1}$ and scalar spectral index $n_s = 0.968$.

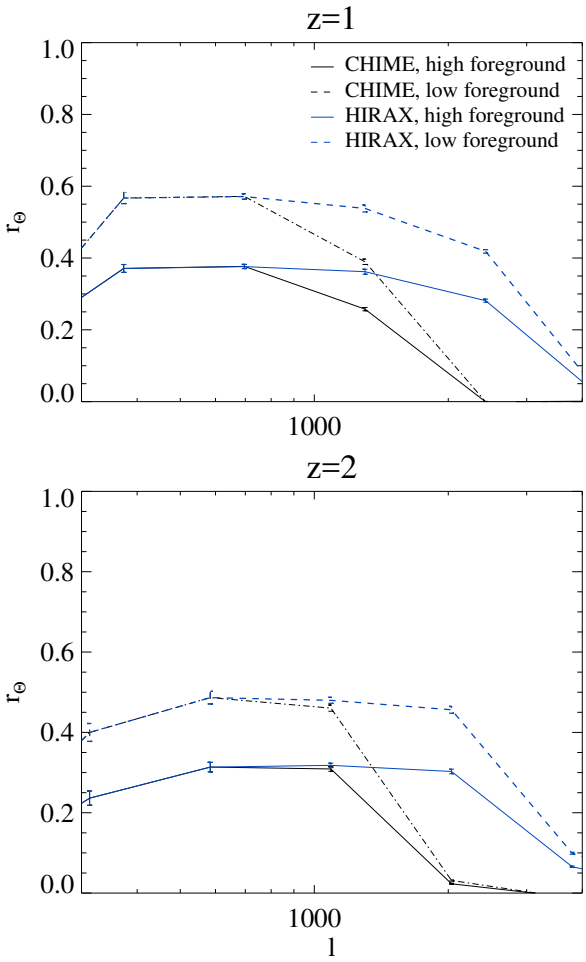

FIG. 5: The correlation coefficient r (Eq.(3) between real kSZ and 21cm IM reconstructed kSZ. Forecasts for two different telescopes and levels of mode loss due to foreground filtering are calculated at $z = 1$ (above) and $z = 2$ (below). The parameters are given in Table.I.

The simulated density and velocity fields at $z = 1$ and 2 are output and used to generate the real kSZ signal. The density fields are then appropriately treated by instrumental effects, as discussed in Section III and Table .I, to imitate realistic fields resolved from 21 cm IM.

Following the procedure demonstrated in Fig.1, we solve for the large scale modes for density fields with tidal reconstruction algorithm. We use the input density fields following our most conservative estimates, namely $R_\parallel = 15$ Mpc/h, $k_{\max} = 0.6$ h/Mpc, $\ell_{\min} = 200$ for $z = 1$, and $R_\parallel = 10$ Mpc/h, $k_{\max} = 0.4$ h/Mpc, $\ell_{\min} = 200$ for $z = 2$.

The restored large scale modes in density fields are used to linearly calculate radial velocity fields v_z. The results for the cross-correlation between calculated v_z and the real v_z, which is output by the simulation, are demonstrated in Fig.3. Important modes for velocity fields (within red line of Fig.2, lower label) are well reproduced by the reconstruction and produce a cross-correlation coefficient greater than 0.7.

We then proceed to a reconstructed kSZ signal by com-

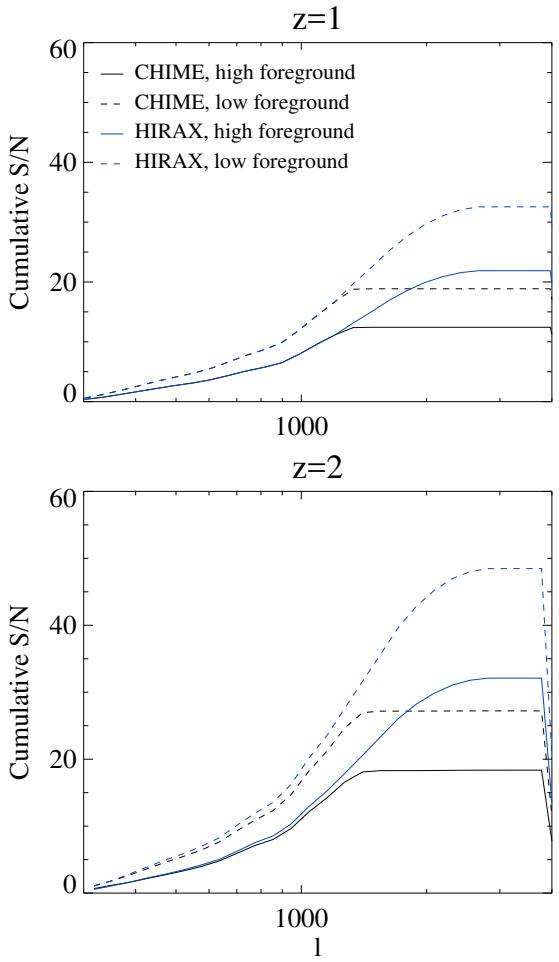

FIG. 6: Cumulative S/N, assuming Planck noise at 217 GHz, $f_{sky} = 0.8$.

bining the reconstructed velocity field with density fields of various conditions. Their correlation coefficients with the exact kSZ are shown in Fig.5. Even with an identical tidal reconstructed velocity field, better foreground removal techniques can improve the correlation coefficient by 0.2. Of course better foreground removal will also provide more modes on which the tidal reconstruction can act. Also, greater angular resolution of telescope will improve the reconstruction at high ℓ.

VII. STATISTICAL ERROR AND S/N

In this Section, we consider our ability to distinguish the kSZ effect from the primary CMB and instrumental noise. We estimate the signal-to-noise for the kSZ effect as:

$$\frac{S}{N} = \frac{C_\ell}{\Delta C_\ell} \simeq r\sqrt{(2\ell+1)\Delta l f_{\rm sky}}\sqrt{\frac{C_\ell^{\rm kSZ,\Delta z}}{C_\ell^{\rm CMB}+C_\ell^{\rm kSZ}+C_\ell^{\rm CMB,N}}}, \quad (10)$$

where $C_\ell^{\rm CMB}$ is the angular power spectrum of primary CMB, $C_\ell^{\rm CMB,N}$ is the contribution to the covariance from instrumental noise, $C_\ell^{\rm kSZ,\Delta z}$ is the kSZ signal from within a certain redshift bin, r is the correlation coefficient defined in Eq.(3), and $f_{\rm sky}$ is the percent of sky area covered by both the CMB and 21 cm IM surveys.

Notice that the S/N is related to the cross correlation coefficient we could obtain from 21cm IM and the relative strength of kSZ signals as opposed to primary CMB and facility noise.

In this paper, $C_\ell^{\rm CMB}$ is calculated using CAMB [25]. $C_\ell^{\rm CMB,N}$ is estimated with Planck data [23] at 217GHz, with sensitivity per beam solid angle given by $\sigma_{p,T} = 8.7\mu K_{\rm CMB}$ and an effective beam full-width-half-maximum of $\theta_{\rm FWHM} \sim 5'$. We assume sky coverage $f_{\rm sky} = 0.8$. $C_\ell^{\rm kSZ,\Delta z}$ is calculated within two bins of size 1200 Mpc/h, centered at redshift 1 & 2, respectively. The cumulative S/N calculated using Eq. (10) is shown in Fig.6. The S/N at $z = 2$ is higher than $z = 1$ due to the high electron density, and the overall S/N should well reach 50 with HIRAX. With Planck noise levels, the resolution of HIRAX already covers the most important ℓ.

VIII. CONCLUSION

In this paper, we have discussed a method for of cross-correlating the kSZ signal with 21 cm IM, a probe which is directly sensitive to the large-scale distribution of baryons. All of the calculations presented here are based on ongoing experiment conditions and realistic noise levels. The loss of large scale modes due to foreground cleaning is identified as the main challenge for obtaining reasonable cross correlation. To alleviate the problem, an algorithm that exploits the non-linear tidal coupling between scales is employed. It could retrieve $> 70\%$ information of the large scale modes. With the reconstructed large scale modes, the velocity fields could be linearly calculated and coupled to density fields to generate a mock kSZ map. The tightness of the correlation between the mock kSZ map and real kSZ is directly related to the S/N we could obtain in real observations.

With existing Planck data, it is reasonable to expect a S/N of at least ~ 15 at redshift 2 with data from CHIME, and HIRAX will yield 50 S/N due to the increased small-scale resolution provided by longer baselines.

The next step for achieving better correlation is to retrieve the low k_z, high $k_\perp$ modes in density fields which are also lost in foregrounds. These modes are supposed to couple with $v_z(\text{low}k_z, \text{low}k_\perp)$ and generate a great percentage of kSZ signals. Unfortunately, the high $k_\perp$ region is beyond the effective scale of tidal reconstruction. However, data from weak lensing and photo-z galaxy surveys, which contain only large-scale structure in the z direction, may probably be use to compensate for the loss.

Cross-correlating the kSZ signal with 21 cm IM is promising due to its feasibility with near-term data and model independence. CHIME is about to start collecting data, and construction for HIRAX is under way, given the reported experiment timelines. It is reasonable to expect our method to be testable

within the next five years. Moreover, the method does not rely on assumptions about velocity fields or the conditions of the interstellar medium, and therefore the results can be more easily understood. We expect our method to be useful tool for studying the baryon distribution up to redshift 2 or higher. Furthermore, the unique property of 21 cm IM of having both large sky coverage and accurate redshift information offers extra information into the diffuse baryonic structure at angular scales of $\ell \sim 1000 - 2000$, larger scales than probed by all the other similar methods proposed. This will foster understanding of stellar feedback at the scale of galaxy clusters and filaments and therefore the evolution of the large-scale structure.

IX. ACKNOWLEDGEMENTS

We acknowledge discussions Wenkai Hu, Tianxiang Mao and Jiawei Shao. The simulations were performed on the BGQ supercomputer at the SciNet HPC Consortium. SciNet is funded by: the Canada Foundation for Innovation under the auspices of Compute Canada; the Government of Ontario; the Ontario Research Fund – Research Excellence; and the University of Toronto. Research at the Perimeter Institute is supported by the Government of Canada through Industry Canada and by the Province of Ontario through the Ministry of Research & Innovation. The Dunlap Institute is funded through an endowment established by the David Dunlap family and the University of Toronto.

[1] U.-L. Pen, ApJ **510**, L1 (1999), astro-ph/9811045.
[2] A. M. Sołtan, A&A **460**, 59 (2006), astro-ph/0604465.
[3] R. A. Sunyaev and Y. B. Zeldovich, Comments on Astrophysics and Space Physics **4**, 173 (1972).
[4] R. A. Sunyaev and I. B. Zeldovich, MNRAS **190**, 413 (1980).
[5] E. T. Vishniac, ApJ **322**, 597 (1987).
[6] M. Fukugita and P. J. E. Peebles, ApJ **616**, 643 (2004), astro-ph/0406095.
[7] N. Hand, G. E. Addison, E. Aubourg, N. Battaglia, E. S. Battistelli, D. Bizyaev, J. R. Bond, H. Brewington, J. Brinkmann, B. R. Brown, et al., Physical Review Letters **109**, 041101 (2012), 1203.4219.
[8] J. Shao, P. Zhang, W. Lin, Y. Jing, and J. Pan, MNRAS **413**, 628 (2011), 1004.1301.
[9] M. Li, R. E. Angulo, S. D. M. White, and J. Jasche, MNRAS **443**, 2311 (2014), 1404.0007.
[10] J. C. Hill, S. Ferraro, N. Battaglia, J. Liu, and D. N. Spergel, ArXiv e-prints (2016), 1603.01608.
[11] S. Ferraro, J. C. Hill, N. Battaglia, J. Liu, and D. N. Spergel, ArXiv e-prints (2016), 1605.02722.
[12] K. Bandura, G. E. Addison, M. Amiri, J. R. Bond, D. Campbell-Wilson, L. Connor, J.-F. Cliche, G. Davis, M. Deng, N. Denman, et al., in *Society of Photo-Optical Instrumentation Engineers (SPIE) Conference Series* (2014), vol. 9145 of *Society of Photo-Optical Instrumentation Engineers (SPIE) Conference Series*, p. 22, 1406.2288.
[13] Y. Xu, X. Wang, and X. Chen, ApJ **798**, 40 (2015), 1410.7794.
[14] http://www.acru.ukzn.ac.za/ hirax/.
[15] U.-L. Pen, R. Sheth, J. Harnois-Deraps, X. Chen, and Z. Li, ArXiv e-prints (2012), 1202.5804.
[16] H.-M. Zhu, U.-L. Pen, Y. Yu, X. Er, and X. Chen, ArXiv e-prints (2015), 1511.04680.
[17] T. Di Matteo, B. Ciardi, and F. Miniati, MNRAS **355**, 1053 (2004), astro-ph/0402322.
[18] K. W. Masui, E. R. Switzer, N. Banavar, K. Bandura, C. Blake, L.-M. Calin, T.-C. Chang, X. Chen, Y.-C. Li, Y.-W. Liao, et al., ApJ **763**, L20 (2013), 1208.0331.
[19] E. R. Switzer, T.-C. Chang, K. W. Masui, U.-L. Pen, and T. C. Voytek, ApJ **815**, 51 (2015), 1504.07527.
[20] K. W. Masui, E. R. Switzer, N. Banavar, K. Bandura, C. Blake, L.-M. Calin, T.-C. Chang, X. Chen, Y.-C. Li, Y.-W. Liao, et al., ApJ **763**, L20 (2013), 1208.0331.
[21] E. R. Switzer, K. W. Masui, K. Bandura, L.-M. Calin, T.-C. Chang, X.-L. Chen, Y.-C. Li, Y.-W. Liao, A. Natarajan, U.-L. Pen, et al., MNRAS **434**, L46 (2013), 1304.3712.
[22] J. R. Shaw, K. Sigurdson, M. Sitwell, A. Stebbins, and U.-L. Pen, Phys. Rev. D **91**, 083514 (2015), 1401.2095.
[23] Planck Collaboration, R. Adam, P. A. R. Ade, N. Aghanim, M. Arnaud, M. Ashdown, J. Aumont, C. Baccigalupi, A. J. Banday, R. B. Barreiro, et al., ArXiv e-prints (2015), 1502.01587.
[24] J. Harnois-Déraps, U.-L. Pen, I. T. Iliev, H. Merz, J. D. Emberson, and V. Desjacques, MNRAS **436**, 540 (2013), 1208.5098.
[25] A. Lewis, A. Challinor, and A. Lasenby, Astrophys. J. **538**, 473 (2000), astro-ph/9911177.